Available online at www.sciencedirect.com
ScienceDirect
Journal of Sound and Vibration 304 (2007) 875–893
JOURNAL OF SOUND AND VIBRATION
www.elsevier.com/locate/jsvi

The influence of damping on the limit cycles for a self-exciting mechanism

J.-J. Sinou*, L. Jézéquel

Laboratoire de Tribologie et Dynamique des Systèmes UMR-CNRS 5513, Equipe Dynamique des Systèmes et des Structures, Ecole Centrale de Lyon, 36 avenue Guy de Collongue, 69134 Ecully Cedex, France

Received 21 July 2006; received in revised form 12 March 2007; accepted 26 March 2007

Abstract

The objective of the present work is to investigate qualitative aspects of mode-coupling instability of self-excited friction-induced oscillations in the presence of structural damping and a cubic nonlinearity. In a previous study, Sinou and Jezequel demonstrated the effects of structural damping in determining stable and unstable zones and indicated that the damping ratio of the coupling modes may be a key factor for avoiding bad design. In this paper, we propose to complete this study by examining the influence of structural damping on limit cycle amplitudes in order to achieve a complete design including not only the evolution of stable/unstable areas but also the evolution of limit cycle amplitudes as functions of the structural damping and nonlinear system parameter. For the sake of simplicity, a two-degree-of-freedom minimal model is constructed and analysed to examine the effects of structural damping and cubic nonlinearity on the limit cycles. The nonlinear behaviour and stable limit cycle amplitudes are determined through a Complex Nonlinear Modal Analysis which makes use of the nonlinear unstable mode governing the nonlinear dynamics of structural systems in unstable areas. Based on this nonlinear modal approach, we will produce and explain qualitative and quantitative results of limit cycle evolutions in the presence of structural damping and nonlinearity.

1. Introduction

Friction-induced vibrations and flutter instability are recognized as one of the most serious problems for industry. Though many researchers have examined the problem of friction-induced vibrations with experimental, analytical and numerical approaches [1–5], there are still no methods for completely eliminating or reducing instability. The addition of damping to one part of a mechanical system such as the pads for brake systems [1,6] is commonly undertaken to reduce or eliminate vibration. While some methodologies propose introducing additional damping to dynamic systems to eliminate or significantly reduce vibrations, it has been demonstrated experimentally and numerically [1,6,7] that the addition of damping may have a detrimental effect. Although a number of studies on damping have been done, it is apparent that the role of damping in flutter instability is not yet fully understood. One of the most

*Corresponding author.
E-mail addresses: jean-jacques.sinou@ec-lyon.fr (J.-J. Sinou), louis.jezequel@ec-lyon.fr (L. Jézéquel).

0022-460X/$ - see front matter © 2007 Elsevier Ltd. All rights reserved.
doi:10.1016/j.jsv.2007.03.043

interesting papers on the influence of damping was published in 1987 by Earles and Chambers [6]. The authors discussed the concept of geometrically induced instability as being the mechanism controlling disc brake squeal and they examined the influence of the physical parameters of the double-pin on a disc system. In particular, they examined the effects of damping and observed that increasing damping not only has a general tendency to decrease instability intensity, but also has the effect of increasing the size of the unstable region for certain physical parameters of the double-pin on a disc system. For example, they observed that increasing the disc damping has little effect on the size of the unstable region, but it reduces the limit cycle amplitudes; however increasing the pin torsional damping reduces the unstable region, but has little effect on the limit cycle amplitudes. They concluded that the role of damping is a complex problem and could not be readily anticipated, and that the varying effects of damping indicate that it is not possible to make predictions intuitively. Recently, an interesting paper by Shin et al. [7] presents the effect of damping on a two-degree-of-freedom model where the disc and the pad are modelled as single modes connected by a sliding friction interface. They clearly indicated that the amount of damping is a key factor. Their analysis suggests that the size of the limit cycles decreases as the damping of both the pad and disc increase simultaneously. Moreover, they found that the damping of the pad and the disc are important in order to avoid unstable vibrations and stick–slip phenomena. They demonstrated that two-degree-of-freedom systems connected through a sliding friction interface can become unstable if damping is added on only one side of the sliding interface.

Recently, some researchers [8,9] have made progress in the analysis of friction-induced instability by studying the influence of structural damping. Hoffmann and Gaul [8] studied the effects of damping on mode-coupling instability in friction-induced oscillations. They demonstrated that linear viscous structural damping changes mode-coupling instability and that an imperfect merging of modes may be observed. They developed a feedback-loop formalism in order to allow a more detailed understanding of the underlying mechanical processes. Nevertheless, they concluded that viscous instability in the field of friction-induced oscillations is in itself a surprising phenomenon. Then, Sinou and Jezequel [9] illustrated the fact that the only effect of adding structural damping is a shift of the curves toward the negative real parts if damping is equally distributed on the two modes involved in the mode coupling phenomenon. Thus, increasing damping increases the critical value of the friction coefficient (i.e. the Hopf bifurcation point) and always stabilizes the brake system. However, if damping is spread non-equally over the two modes, a shifting and a smoothing effect can be seen on coalescence curves. In this case, increasing damping may tend to make the brake system unstable for a lower value of the friction coefficient. They then illustrated the fact that the damping ratio of the coupling modes may be a key factor to be taken into account. They gave the complete analytical expressions of the Hopf bifurcation point that defines the stable/unstable boundary regions via the Routh–Hurwitz criterion and demonstrated that the Hopf bifurcation point depends on the structural damping of the coupling modes, the damping ratio and the frequency ratio between these two modes.

In conclusion, all these recent studies [7–9] indicate that neglecting damping in a stability analysis or adding damping on only one part of the system may result in worse design and lead to a misunderstanding of the mode coupling instability of mechanical systems. Damping therefore appears to be one of the key parameters and may not be ignored in the design of mechanical systems. It is well known that the design of mechanical systems must not be restricted to stability analysis. If the equilibrium solution of the mechanical system is unstable, the nonlinear dynamical behaviour and the limit cycles become the design criterion. This is only due to the fact that even if the equilibrium point is unstable, the associated limit cycles of the mechanical system may be very small and hence the instability could be negligible. Given this fact, we will seek to describe the effects of damping in order to avoid worse design in mechanical systems subject to flutter instability. The main objective of this paper will be to clarify the influence of structural damping on the limit cycles amplitudes. The study is set up as follows: first, the minimal nonlinear two-degrees-of-freedom system of mode-coupling instability in friction-induced vibrations is presented. Second, a brief review of the effects of damping on mode-coupling instability is given. Then, the role of damping on the limit cycles is examined. The influence of practical parameters is also examined. To save time and to extensively cover the parametric studies, the computational methodology of the Complex Nonlinear Modal Analysis is applied [10].

2. Mechanical system and stability analysis

2.1. Description of the two degree of freedom model

Fig. 1 shows the minimal nonlinear two-degrees-of-freedom model to be used in the following. This model has its origins in the model proposed by Hulten [11] in order to study drum brake squeal (flutter instability), and was used by Sinou and Jézéquel [9] in order to study the effects of damping. This minimal two-degrees-of-freedom model is chosen due to its simplicity and to better understand the roles of various physical parameters including, more specifically, damping on the stability of the fixed points and the associated nonlinear behaviour and limit cycle amplitudes. To understand the intrinsic features of the mode-coupling mechanism and the role of damping, it is assumed that the mass and band surfaces are always in contact. The contact between the mass and the band is modelled by two plates supported by two springs, one having a cubic nonlinearity. Considering the friction forces between the two plates and the band, Coulomb's law is assumed $T = \mu N$ where T and N define the tangential and normal forces and μ is the coefficient of friction which is assumed to be constant. For the sake of simplicity, the relative velocities between the band speed and the displacements of the mass are assumed to be positive so that the direction of friction force does not change.

The equations of motion for the present model are given by

$$\begin{bmatrix} 1 & 0 \\ 0 & 1 \end{bmatrix} \begin{pmatrix} \ddot{X}_1 \\ \ddot{X}_2 \end{pmatrix} + \begin{bmatrix} \eta_1\omega_{0,1} & 0 \\ 0 & \eta_2\omega_{0,2} \end{bmatrix} \begin{pmatrix} \dot{X}_1 \\ \dot{X}_2 \end{pmatrix} + \begin{bmatrix} \omega_{0,1}^2 & -\mu\omega_{0,2}^2 \\ \mu\omega_{0,1}^2 & \omega_{0,2}^2 \end{bmatrix} \begin{pmatrix} X_1 \\ X_2 \end{pmatrix} = \begin{pmatrix} -\varphi^{\mathrm{NL}} X_1^3 \\ -\mu\varphi^{\mathrm{NL}} X_1^3 \end{pmatrix}, \tag{1}$$

where $\varphi^{\mathrm{NL}} = k^{\mathrm{NL}}/m$. X_1 and X_2 are the relative displacements indicated in Fig. 1. $\omega_{0,i}$ and η_i define the ith natural frequency $\omega_{0,i} = \sqrt{k_i/m}$ and relative damping coefficient $\eta_i = c_i/\sqrt{k_i m}$, respectively. The values of the physical parameters are given in Table 1.

2.2. Stability analysis

The equations of motion (1) may be rewritten in the form

$$\mathbf{M}\ddot{\mathbf{X}} + \mathbf{C}\dot{\mathbf{X}} + \mathbf{K}\mathbf{X} = \mathbf{F}^{\mathbf{NL}}(\mathbf{X}), \tag{2}$$

where $\mathbf{X} = [\mathbf{X}_1\, \mathbf{X}_2]^{\mathrm{T}}$ defines the displacement response two-dimensional vectors of the degrees-of-freedom. For a nonlinear system, stability is investigated by calculating the eigenvalues of the linearized system at the

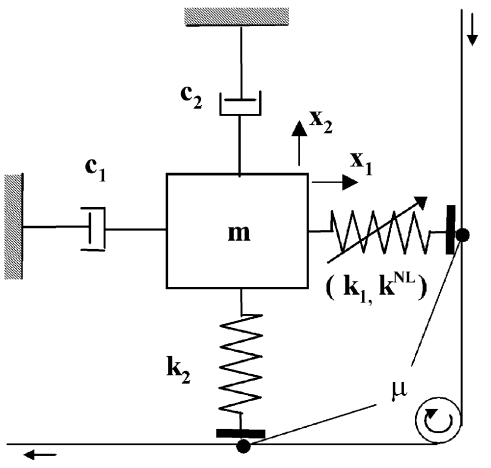

Fig. 1. Two degree-of-freedom model with cubic nonlinearities.

Table 1
Value of the physical parameters

Notation	Description	Value
$\omega_{0,1}$	First natural frequency	$2\pi * 1000\ \mathrm{rad\,s^{-1}}$
$\omega_{0,2}$	Second natural frequency	$2\pi * 800\ \mathrm{rad\,s^{-1}}$
η_1	First relative damping coefficient	0.06
η_2	Second relative damping coefficient	0.06
k^{NL}	Cubic nonlinear term	$10^{11}\mathrm{N\,m^{-3}}$
m	Mass	1 kg
μ	Friction coefficient	0.3

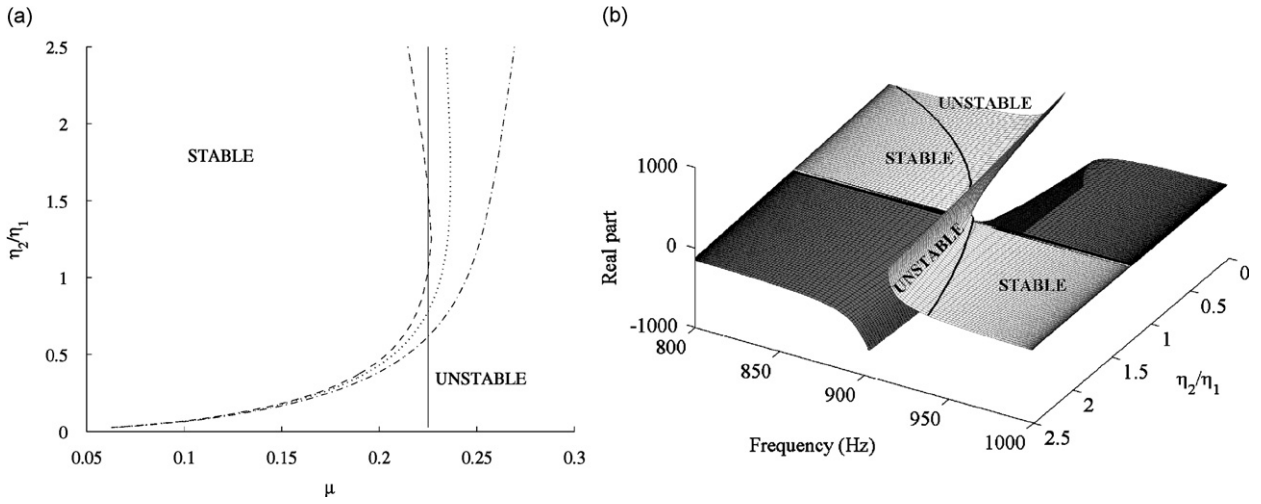

Fig. 2. Effects of the damping on the stability: (a) stable and unstable zones versus the damping ratio η_2/η_1 and the friction coefficient μ ($-$ undamped, $--\eta_1 = 0.02, \cdots \eta_1 = 0.06$, $-.-\eta_1 = 0.1$); (b) evolution of the stable and unstable modes in the complex plane for $\eta_1 = 0.02$.

equilibrium point $\mathbf{X}_0$ [5]

$$\mathbf{M}\ddot{\bar{\mathbf{X}}} + \mathbf{C}\dot{\bar{\mathbf{X}}} + \left(\mathbf{K} + \left.\frac{\partial \mathbf{F}^{\mathrm{NL}}}{\partial \bar{\mathbf{X}}}\right|_{\mathbf{X}_0}\right)\bar{\mathbf{X}} = \mathbf{0}, \tag{3}$$

where $\bar{\mathbf{X}}$ defines small perturbation about the equilibrium point $\mathbf{X}_0$ that is obtained by solving the nonlinear static equations $\mathbf{K}\mathbf{X_0} = \mathbf{F}^{\mathbf{NL}}(\mathbf{X_0})$. For the nonlinear system being studied, the only physical static solution corresponds to the origin of the system (see Appendix A). Then, the stability analysis of the system (2) is given by the linear system $\mathbf{M}\ddot{\bar{\mathbf{X}}} + \mathbf{C}\dot{\bar{\mathbf{X}}} + \mathbf{K}\bar{\mathbf{X}} = \mathbf{0}$ due to the fact that the linearized expression of the nonlinear terms equals zero. So, stability of the system (1) may be investigated by performing an eigenvalue analysis of the characteristic equation

$$\det\begin{vmatrix} \lambda^2 + \eta_1\omega_{0,1}\lambda + \omega_{0,1}^2 & -\mu\omega_{0,2}^2 \\ \mu\omega_{0,1}^2 & \lambda^2 + \eta_2\omega_{0,2}\lambda + \omega_{0,2}^2 \end{vmatrix} = 0, \tag{4}$$

where λ define the eigenvalues of the system. Due to the non-symmetric stiffness matrix (as a result of the friction force), this two-degrees-of-freedom model may become unstable. The mechanical system is stable if all

the real part of the eigenvalues are negative, and unstable if there exist one or more eigenvalues having a positive real part.

Fig. 2(a) shows the results of an eigenvalue analysis of the two-degrees-of-freedom for various structural damping. For the undamped case, the borderline for the transition between the stable and unstable equilibrium points lies close to $\mu = 0.225$. With respect to the control parameter μ, the effects of damping appear to be a very surprising and complex phenomenon. In order to better assess the role of damping, Sinou and Jezequel used the Routh–Hurwitz criterion [9] and demonstrated that the value of the friction coefficient μ_0 (i.e. the control parameter) at the Hopf bifurcation point is given by

$$\mu_0^2 = \frac{\eta_2^2\sqrt{\alpha_\omega}\alpha_\eta(\sqrt{\alpha_\omega}\alpha_\eta + 1)(\alpha_\eta + \sqrt{\alpha_\omega}) + \alpha_\eta(\alpha_\omega - 1)^2}{\sqrt{\alpha_\omega}(\sqrt{\alpha_\omega}\alpha_\eta + 1)^2}, \tag{5}$$

where $\alpha_\omega = \omega_{0,1}/\omega_{0,2}$ and $\alpha_\eta = \eta_1/\eta_2$. This last equation indicates that the effect of damping is more complicated than the commonly accepted idea that ''adding damping always stabilizes the mechanical system''. As previously explained by Hoffmann and Gaul [8], and Sinou and Jézéquel [9], if we consider the case of proportional damping (i.e. $c_1 = c_2$ corresponding in our case to $\eta_2/\eta_1 = \omega_{0,1}/\omega_{0,2} = 1.25$), increasing the value of the proportional damping increases the value of the control parameter at the Hopf bifurcation point μ_0 and the mechanical system is more stable. Physically speaking the frequencies remain constant and the ''lowering of the real part curves'' is obtained [8,9]. Nevertheless, if non-proportional damping is added (i.e. $c_1 \neq c_2$ or $\eta_1\omega_{0,1} \neq \eta_2\omega_{0,2}$), the mechanical system may become more stable but also more unstable.

Finally, Sinou and Jézéquel [9] showed that structural damping not only influences the stability of the mechanical system but also has an important part in defining the value of the unstable frequency. This fact is illustrated in Fig. 2(b). The white surface defines the frequency of the potentially unstable mode if the equilibrium point is unstable (i.e. corresponding to the eigenvalue having a positive real part) whereas the black surface corresponds to the associated stable mode. It is shown that the unstable mode may come from the high or low frequency of the two coupling modes. The borderline between the black and white surfaces corresponds to proportional damping ($c_1 = c_2$ corresponding in our case to $\eta_2/\eta_1 = \omega_{0,1}/\omega_{0,2} = 1.25$).

All these aspects and phenomena indicate that damping plays an important role for mode-coupling type instability in friction induced vibrations. For more detailed aspects and extensive results, we refer the interested reader to the papers of Hoffmann and Gaul [8] and Sinou and Jézéquel [9].

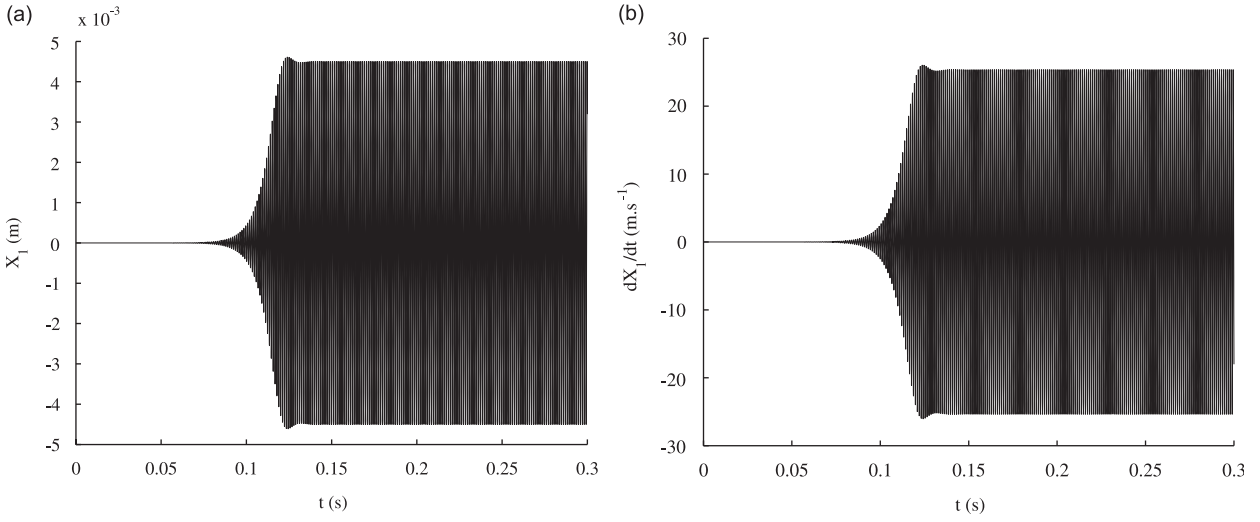

Fig. 3. Evolution of the displacement $X_1(t)$ and velocity $\dot{X}_1(t)$ (for $\mu = 0.25$ and $\eta_1 = \eta_2 = 0.06$): (a) displacement $X_1(t)$, (b) velocity $\dot{X}_1(t)$.

3. Nonlinear behaviour of the mechanical system

3.1. Self-excited oscillations and stable limit cycles

While the determination of the eigenvalues is useful in evaluating the effect of damping on stable and unstable zones, it cannot evaluate the vibration amplitudes if the equilibrium point of the mechanical system is unstable. If stable limit cycles exist, the limit cycle amplitudes and the time-history solutions of the nonlinear equations can be calculated by using the classic fourth-order Runge–Kutta algorithm. For example, Figs. 3 show the transient response analysis and the predicted nonlinear vibration amplitudes of the displacement $X_1(t)$ and the velocity $\dot{X}_1(t)$ (for $\mu = 0.25$ and $\eta_1 = \eta_2 = 0.06$). The displacements and velocities increase until the periodic self-excited oscillations of the nonlinear dynamical behaviour of the system are obtained. Nevertheless, this procedure is rather expensive and consumes considerable resources both in terms of the computation time and in terms of the data storage requirements. So in order to undertake extensive parametric studies and to investigate the role of structural damping, nonlinear methods can be applied to find the nonlinear response of the dynamical system. Because the purpose of this section is to study the effect of damping on limit cycle amplitudes of the nonlinear system, we refer the interested reader to the following references for an extensive overview of the various nonlinear methods and approaches [5,12].

Before briefly describing the methodology of this nonlinear modal approach that will be used in this paper, it may be observed that the principle of this method is based on the well-known technique of equivalent linearization of Krylov and Bogoliubov [13]: the idea is to replace the nonlinear system by an equivalent linear system in which the difference between the two systems is minimized. Then, the solution of the associated linear system is taken as an approximation of the original nonlinear problem by considering only one harmonic for the final periodic solution. In order to obtain the complex and exact solution that can consists of more than one harmonic (see for example the study of D'Souza and Dweib [14] where the nonlinear self-excited vibrations consists of a steady-state component, a component oscillating at the fundamental frequency, and a second harmonic component) which is not the purpose of this nonlinear modal approach, other nonlinear methods [5,12] such the methodology developed by D'Souza and Dweib [14] may be used.

3.2. Complex Nonlinear Modal Analysis

3.2.1. Limit cycles determination

In this study, the Complex Nonlinear Modal Analysis [10] will be used in order to obtain the approximated limit cycles of the nonlinear mechanical system. We do not claim to make an important contribution in this section of the paper: the purpose here is to give a brief overview of the Complex Nonlinear Modal Analysis. We refer the interested reader to Ref. [10] for an extensive explanation of this nonlinear modal method.

First, the nonlinear equations of the system are rewritten in state variables $\mathbf{Y} = [X_1\, X_2\, \dot{X}_1\, \dot{X}_2]^{\mathrm{T}}$:

$$\dot{\mathbf{Y}} = \mathbf{A}\mathbf{Y} + \mathbf{FNL}(\mathbf{Y}), \tag{6}$$

where $\mathbf{A}$ is a 4×4 matrix containing the mass, damping and stiffness parameters of the mechanical system. $\mathbf{FNL}(\mathbf{Y})$ is the vector containing the nonlinear cubic expressions of the nonlinear system defined in Eq. (1).

The idea of the Complex Nonlinear Modal Analysis is to consider that the nonlinear behaviour of the system may be approximated by studying only the modal participation of the unstable modes if the equilibrium point of the mechanical system is unstable. It is assumed that all modal participation of the stable modes (associated with the eigenvalues having negative real part $\mathrm{Re}(\lambda) < 0$) is negligible in regard to the unstable mode (associated with the eigenvalues having positive real part $\mathrm{Re}(\lambda) > 0$). When the nonlinear system becomes unstable, Eq. (6) is first governed by the approximated increasing unstable curve

$$\tilde{\mathbf{Y}}(t) = \Psi \mathrm{e}^{\lambda t} + \bar{\Psi} \mathrm{e}^{\bar{\lambda} t}, \tag{7}$$

where λ and $\bar{\lambda}$ are the complex eigenvalues of equivalent linear system at the equilibrium point having positive real part (associated with the unstable mode) and $\Psi$and $\bar{\Psi}$ are the associated eigenvectors.

Then, when the increasing curve of the system becomes the limit cycle, Eq. (7) defines the stable periodic approximated solution $\tilde{\mathbf{Y}}$ depending only on the pair of purely imaginary eigenvalues $\lambda = -\bar{\lambda} = \mathrm{i}\omega_1$

(i.e. $\mathrm{Re}(\lambda)=0$) with the associated normalized eigenvector $\Psi=\Psi_1$ and conjugated normalized eigenvector $\bar{\Psi}=\bar{\Psi}_1$:

$$\tilde{\mathbf{Y}}(t)=p(\Psi_1 e^{i\omega_1 t}+\bar{\Psi}_1 e^{-i\omega_1 t}), \tag{8}$$

where p is the amplitude of the periodic approximated solution governed by the unstable mode. It may be observed that the change from instability to stability of the self-exciting vibrations that indicates the limit cycle, is obtained when the real parts λ and $\bar{\lambda}$ equal zero. The approximated solution $\tilde{\mathbf{Y}}(t)$ considers only the modal participation of the unstable mode.

So, the objective of the Complex Nonlinear Modal Analysis is to determine the amplitude p of the periodic approximated solution, the associated frequency ω_1 and the associated eigenvector Ψ_1. It may be observed that no assumption is made about the value of the control parameter and more particularly that the limit cycle amplitudes may be estimated far from the Hopf bifurcation point. Moreover, the method may be applied to estimate stable or semi-stable limit cycles.

Considering the eigenvalues of the linearized system of Eq. (1), the real part of eigenvalues defines the growth rates of the vibrations until the periodic self-excited oscillations of the system are reached. When the periodic oscillations are obtained, two eigenvalues (λ and $\bar{\lambda}$) have their real part equal to zero (i.e. $\mathrm{Re}(\lambda)=0$) whereas all the other eigenvalues have negative real part (i.e. $\mathrm{Re}(\lambda)<0$). The purpose of the Complex Nonlinear Modal Analysis is to be able to follow the evolution of the real parts of eigenvalues from the unstable equilibrium point (defined for $p=0$) to the periodic oscillations. It may be observed that the initial value for the determination of the limit cycles is given by $p=\Delta p$. Then, from the equilibrium point to the periodic oscillations, the unstable approximated solution curve $\tilde{\mathbf{Y}}(t,p)$ for a given value of p is defined by

$$\tilde{\mathbf{Y}}(t,p)=p(\Psi_1(p)e^{\lambda(p)t}+\bar{\Psi}_1(p)e^{\bar{\lambda}(p)t}). \tag{9}$$

The evolution of the eigenvalues $\lambda(p)$ and the associated normalized eigenvector $\Psi_1(p)$ are obtained by determining the eigenvalues and associated eigenvectors of the equivalent linear system of the nonlinear system defined in Eq. (6). This is done by using the concept of the equivalent linearization procedure [15,16]. The principle of the linearized equivalent approach is based on the idea of finding a linear system which is equivalent to the nonlinear system at the unstable fixed point

$$\dot{\tilde{\mathbf{y}}}=\mathbf{A}\tilde{\mathbf{y}}+\mathbf{FNL}(\tilde{\mathbf{y}})\approx\mathbf{A}\tilde{\mathbf{y}}+\mathbf{A}_{\mathbf{FNL}}\tilde{\mathbf{y}}=\mathbf{A}_{\mathbf{equi}}\tilde{\mathbf{y}}, \tag{10}$$

where $\mathbf{A}_{\mathbf{FNL}}$ defines the equivalent linear system of the nonlinear terms $\mathbf{FNL}(\tilde{\mathbf{y}})$. $\tilde{\mathbf{y}}$ defines the associated periodic solution of oscillations $\tilde{\mathbf{Y}}(t,p)$. The expression of $\tilde{\mathbf{y}}(t,p)$ is given by

$$\tilde{\mathbf{y}}(t,p)=p(\Psi_1(p)e^{i\omega(p)t}+\bar{\Psi}_1(p)e^{-i\omega(p)t}), \tag{11}$$

where $\omega(p)$ is the frequency of the periodic solution and corresponds to the imaginary part of the eigenvalue $\lambda(p)$. The equivalent linear system that is defined in Eq. (10) and the associated matrix $\mathbf{A}_{\mathbf{FNL}}$ are obtained such that the difference ε between the equivalent linear and nonlinear systems

$$\varepsilon\equiv\mathbf{FNL}(\tilde{\mathbf{y}})-\mathbf{A}_{\mathbf{FNL}}\tilde{\mathbf{y}} \tag{12}$$

is minimized for every of $\tilde{\mathbf{y}}(t,p)$ of the form defined by Eq. (11). Using the least square method, the minimization is performed according to the criterion $\mathrm{Min}(\int_0^{2\pi/\omega(p)}\varepsilon^T\varepsilon\,dt)$. Finally, the evolution of the eigenvalues $\lambda(p)$ and the associated normalized eigenvector $\Psi_1(p)$ are obtained by determining the eigenvalues and associated eigenvectors of $\mathbf{A}_{\mathbf{equi}}$.

The periodic approximated oscillations are obtained by incrementing the value of p until two eigenvalues $\lambda(p)$ of $\mathbf{A}_{\mathbf{equi}}$ have their real part equal to zero whereas all the other eigenvalues have negative real part. For each increment of p, we calculate the linear equivalent system, the eigenvalues $\lambda(p)$ and the associated normalized eigenvectors $\Psi(p)$. In numerical practice, it may be difficult to obtain the exact value of the final amplitude p and the change of the sign of the real parts of eigenvalues, indicating a change of oscillations from stability to instability (or vice versa) and the perfect detection of the neutral stability of oscillations, defining the periodic self-exciting vibrations. So, the value of the increment δp of the amplitude p may be sufficiently

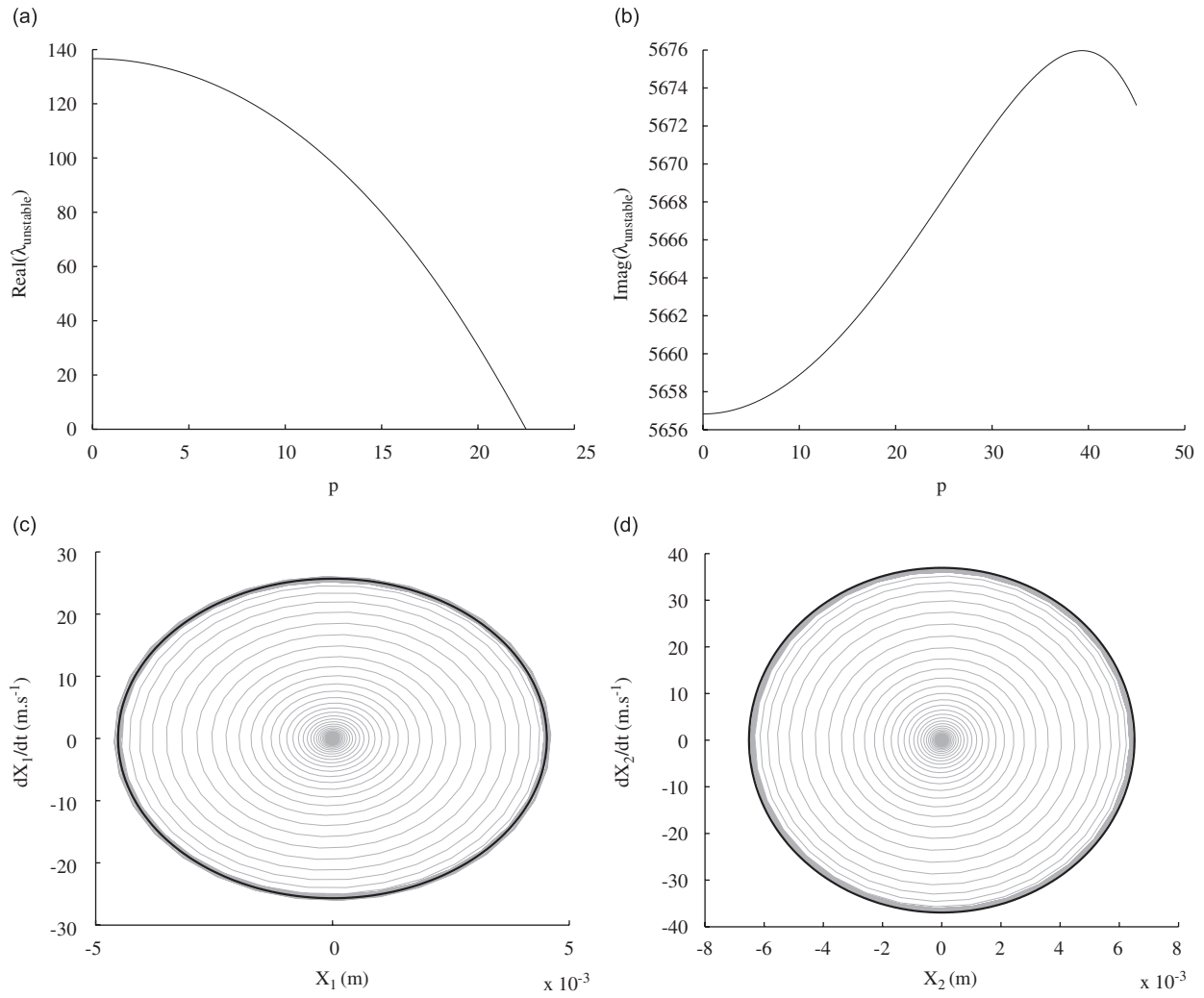

Fig. 4. Evolutions of the unstable mode and the associated limit cycles for $\mu = 0.25$ and $\eta_1 = \eta_2 = 0.06$ (greyline: Runge–Kutta 4, blackline: nonlinear modal analysis): (a) real parts, (b) associated imaginary part, (c) limit cycle $(X_1, \dot{X}_1)$, and (d) limit cycle $(X_2, \dot{X}_2)$.

small. In the cases of stable limit cycles, a final correction using a linear extrapolation follows the estimation of the final amplitude p to exactly define the neutral stability of oscillations indicating the limit cycle.

In order to illustrate the usefulness and efficiency of this nonlinear modal approach, the previous numerical example is considered (see Fig. 3). Figs. 4(a) and (b) show the numerical evolution of the real part of the unstable mode and the associated evolution of the imaginary part which describes the frequency of the unstable mode. As illustrated in Fig. 4(a), the real part of the unstable mode decreases from the original positive value (obtained by performing an eigenvalue analysis of the characteristic Eq. (4)) to zero. Then, Figs. 4(c) and (d) illustrate the associated limit cycles. The grey lines illustrate the convergence of the trajectory to the limit cycle by using direct numerical integration (as previously indicated in Fig. 3 for the displacement $X_1(t)$ and the velocity $\dot{X}_1(t)$) with initial conditions around zero. It appears that the classic fourth-order Runge–Kutta algorithm and the nonlinear modal approach agree quite well.

Moreover, Table 2 give a comparison of the computational times required for the convergence of the trajectory to the limit cycles by using direct numerical integration (Runge–Kutta method) and the proposed technique of Complex Nonlinear Modal Analysis. It clearly demonstrates the advantage of the proposed method.

Table 2
Comparison of the computational times (CPU time) required by using the direct numerical integration (Runge–Kutta method) and the proposed technique of Complex Nonlinear Modal Analysis

μ	η_1	η_2	Runge–Kutta method	Proposed technique
0.25	0.06	0.06	0.89	0.21
0.3	0.02	0.025	0.93	0.09
0.3	0.06	0.075	0.91	0.22
0.3	0.09	0.1125	0.86	0.10
0.3	0.12	0.15	0.89	0.18
0.3	0.12	0.225	1.54	0.13
0.3	0.06	0.1125	0.82	0.09
0.3	0.06	0.0562	0.91	0.24
0.3	0.12	0.1125	0.87	0.18

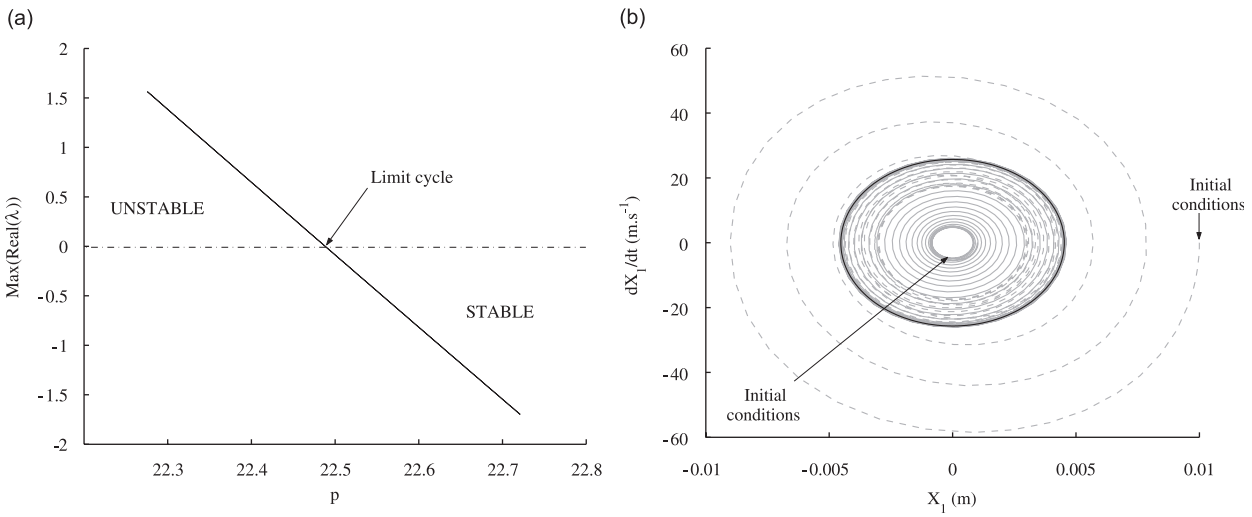

Fig. 5. Stability curve of the limit cycles and comparison/validation with the estimation of limit cycles via the Runge–Kutta integration (for $\mu = 0.25$ and $\eta_1 = \eta_2 = 0.06$) (greyline: Runge–Kutta 4, blackline: nonlinear modal analysis): (a) evolution of the real part, (b) limit cycles $(X_1, \dot{X}_1)$.

3.2.2. Stability of the limit cycle

Once a limit cycle is found, several methods exist to investigate the stability of periodic oscillations: for example, the stability of periodic solutions may be determined using Lyapunov functions [12]. Moreover, the stability of periodic solution may be carried out by using frequential methods based on a perturbation in the time domain applied to the known harmonic solution [17].

As discussed in Ref. [18], limit cycle stability can be determined by considering the evolution of eigenvalues: by applying a small perturbation Δp to the estimated amplitude p of the final periodic approximated solution $\tilde{\mathbf{y}}(t,p)$ and by considering the associated evolutions of the frequency $\omega(p+\Delta p)$ and $\Psi_1(p+\Delta p)$, the stability of the periodic approximated solution may be studied by observing the variation of the real part of eigenvalues of the matrix $\mathbf{A}_{\mathbf{equi}}$ caused by the perturbation Δp. In this study, the equilibrium point is unstable until $\mathbf{A}_{\mathbf{equi}}$ has two eigenvalues with zero real parts and all the others having negative real parts. So, the stability of the limit cycle may be restricted to the two following cases:

- If all eigenvalues of $\mathbf{A}_{\mathbf{equi}}$ have negative real parts for $p+\Delta p$ and some eigenvalue(s) have positive real parts for $p-\Delta p$ (where Δp is a small positive perturbation), the limit cycle is stable.
- If some eigenvalue(s) of $\mathbf{A}_{\mathbf{equi}}$ have positive real parts for $p+\Delta p$ and $p-\Delta p$, the limit cycle is semi-stable.

In order to study the stability of the estimated limit cycles on the previous physical case, a small variation is applied to the predicted amplitude p. In Fig. 5(a), the stability of limit cycles is illustrated by using the Complex Nonlinear Modal Analysis (for $\mu = 0.25$, $\eta_1 = \eta_2 = 0.06$). It may be observed that the maximum real part of eigenvalues changes from a positive value to a negative value. When the real part is equal to zero, the neutral stability of self-exciting oscillations takes place and the limit cycles appear. The limit cycles are stable and there is agreement between the estimations given by time domain simulations and the nonlinear modal analysis (see Figs. 3 and 5(b) for two different initial conditions).

3.3. Effects of damping on the limit cycles

To further our understanding of the effects of damping on limit cycles, two physical cases will be studied: the first case considers proportional damping ($c_1 = c_2$, i.e. $\omega_{0,1}\eta_1 = \omega_{0,2}\eta_2$) and the second non-proportional damping ($c_1 \neq c_2$, i.e. $\omega_{0,1}\eta_1 \neq \omega_{0,2}\eta_2$). The evolution of the limit cycles versus damping will be studied by applying the Complex Nonlinear Modal Analysis.

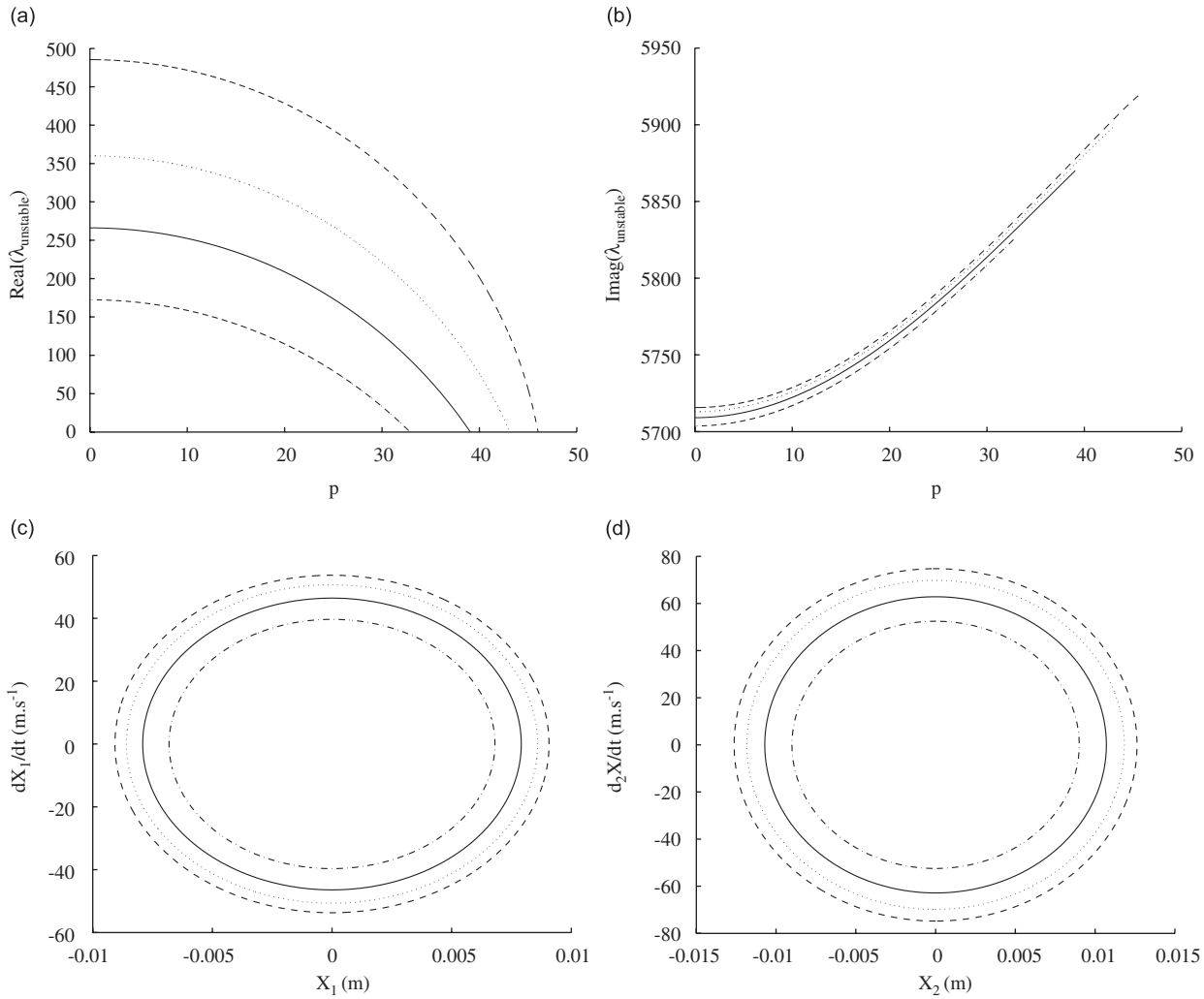

Fig. 6. Evolutions of the unstable mode and the associated limit cycles for $\mu = 0.3$ and $k^{NL} = 10^{11}\,\mathrm{N\,m^{-3}}$ with proportional structural damping ($--$ $c_1 = c_2 = 125.7\,\mathrm{Nm^{-1}s^{-1}}$, $\cdots$ $c_1 = c_2 = 377\,\mathrm{Nm^{-1}s^{-1}}$, $-$ $c_1 = c_2 = 565.5\,\mathrm{Nm^{-1}s^{-1}}$, $-.-$ $c_1 = c_2 = 754\,\mathrm{Nm^{-1}s^{-1}}$): (a) real parts, (b) associated imaginary part, (c) limit cycles $(X_1, \dot{X}_1)$, and (d) limit cycles $(X_2, \dot{X}_2)$.

Table 3
Proportional structural damping

Case	Symbol	η_1	η_2	c_1 ($\mathrm{Nm^{-1}s^{-1}}$)	c_2 ($\mathrm{Nm^{-1}s^{-1}}$)
1	−−	0.02	0.025	125.7	125.7
2	···	0.06	0.075	377	377
3	−	0.09	0.1125	565.5	565.5
4	−.−	0.12	0.15	754	754

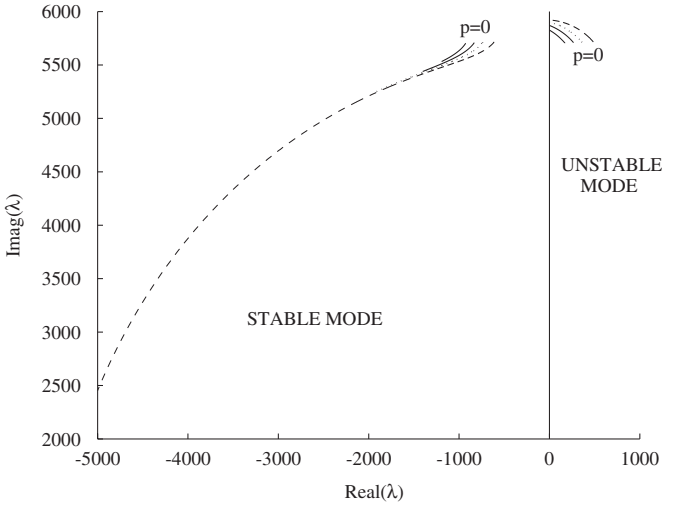

Fig. 7. Evolution of the stable and unstable modes in the complex plane with proportional structural damping (−− $c_1 = c_2 = 125.7\,\mathrm{Nm^{-1}s^{-1}}$, ··· $c_1 = c_2 = 377\,\mathrm{Nm^{-1}s^{-1}}$, − $c_1 = c_2 = 565.5\,\mathrm{Nm^{-1}s^{-1}}$, −.− $c_1 = c_2 = 754\,\mathrm{Nm^{-1}s^{-1}}$).

3.3.1. Proportional damping

Firstly, we will study the effect of increasing the damping coefficients by keeping proportional damping (i.e. $c_1 = c_2$ or $\eta_1\omega_{0,1} = \eta_2\omega_{0,2}$). Figs. 6(a) and (b) show the results of the evolution of the real part and imaginary part of the unstable mode corresponding to four values of proportional damping that are given in Table 3. Figs. 6(c) and (d) show the associated limit cycles. In these cases, the well known role of damping is recovered: it is obvious that increasing proportional damping decreases the limit cycle amplitudes $(X_1, \dot{X}_1)$ and $(X_2, \dot{X}_2)$. Physically speaking, this may be explained by the fact that the growth rates of the equilibrium point (for $p = 0$) is altered by a certain amount depending on proportional damping, whereas the merging-scenario is unchanged. Intuitively, increasing the proportional damping decreases the growth rates by "lowering the real part curves", and the energy of mode coupling instability has to overcome the nonzero structural energy dissipation before generating self-excited oscillations and limit cycles. Therefore the more damped the mechanical system is, the lower the limit cycle amplitudes are (if these limit cycle are stable).

Moreover, Fig. 7 illustrates the evolution of the two complex eigenvalues of the unstable and the associated stable modes. It may be observed that the two modes merge at $p = 0$ due to proportional damping (i.e. the stable and unstable modes have the same frequency). Then, the real parts of the stable and unstable modes decrease until the periodic self-excited oscillations.

Moreover, it is calculated that the limit cycles are stable by using the Complex Nonlinear Modal Analysis, as previously explained in Section 3.2.2.

3.3.2. Non-proportional damping

Now the effects of non-proportional damping will be investigated by considering the ratios of non-proportional damping $c_1/c_2 = 1.5$ and $c_1/c_2 = 0.75$ as indicated in Table 4. Fig. 8 show the evolutions of the

Table 4
Non-proportional structural damping

Case	Symbol	η_1	η_2	c_1 ($\mathrm{Nm^{-1}s^{-1}}$)	c_2 ($\mathrm{Nm^{-1}s^{-1}}$)
1	−−	0.12	0.225	754	1131
2	···	0.06	0.1125	377	565.5
3	−	0.06	0.0562	377	282.75
4	−.−	0.12	0.1125	754	565.5

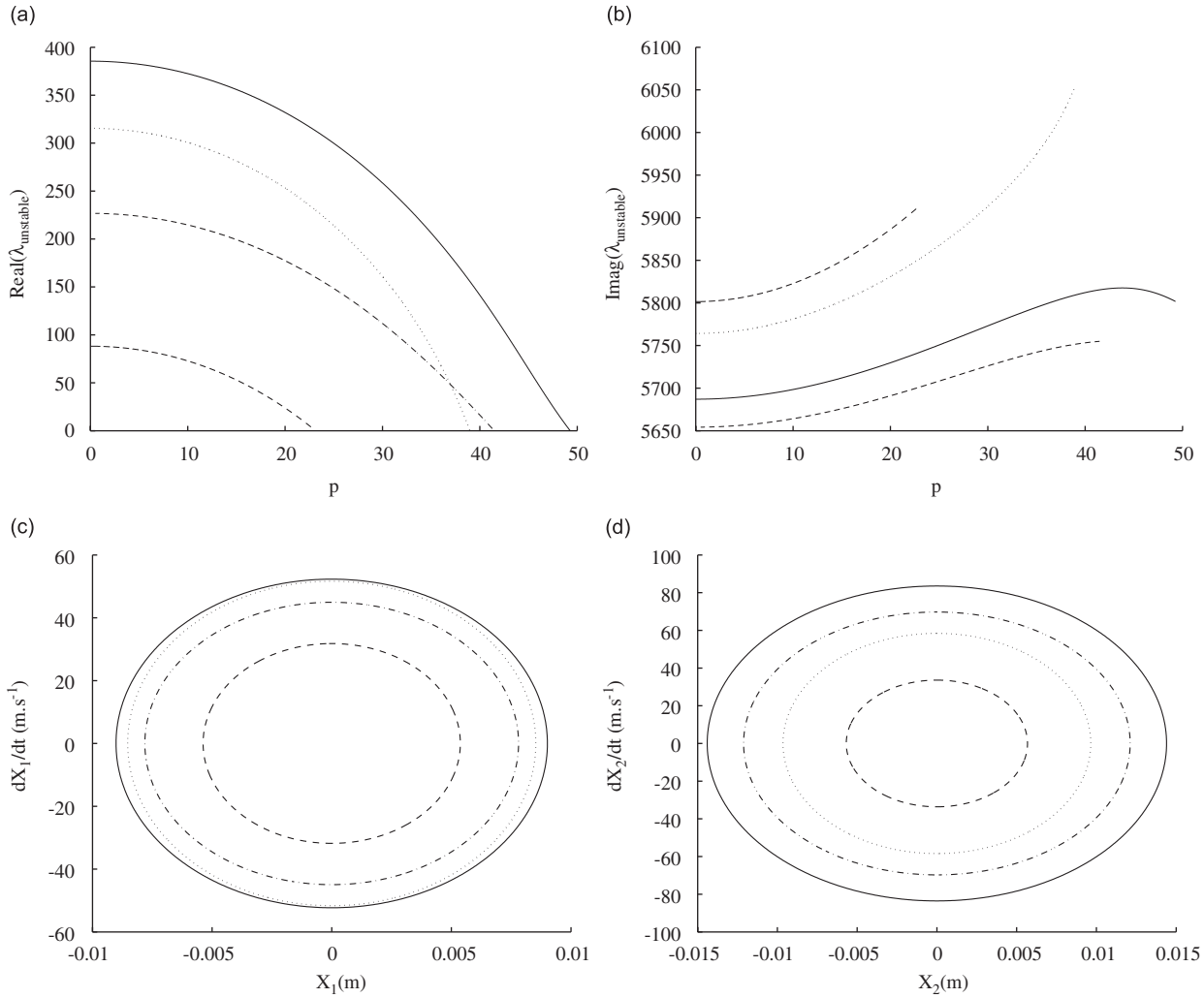

Fig. 8. Evolutions of the unstable mode and the associated limit cycles for $\mu = 0.3$ and $k^{\mathrm{NL}} = 10^{11}\,\mathrm{N\,m^{-3}}$ with non-proportional structural damping (− − $c_1 = 754\,\mathrm{Nm^{-1}s^{-1}}$ and $c_2 = 1131\,\mathrm{Nm^{-1}s^{-1}}$, ··· $c_1 = 377\,\mathrm{Nm^{-1}s^{-1}}$ and $c_2 = 565.5\,\mathrm{Nm^{-1}s^{-1}}$, − $c_1 = 377\,\mathrm{Nm^{-1}s^{-1}}$ and $c_2 = 282.75\,\mathrm{Nm^{-1}s^{-1}}$, −.− $c_1 = 754\,\mathrm{Nm^{-1}s^{-1}}$ and $c_2 = 565.5\,\mathrm{Nm^{-1}s^{-1}}$): (a) real parts, (b) associated imaginary part, (c) limit cycles $(X_1, \dot{X}_1)$, and (d) limit cycles $(X_2, \dot{X}_2)$.

real and imaginary parts of the unstable mode and the associated limit cycles. Fig. 9 illustrates the evolution of the stable and unstable modes in the complex plane. As previously explained, it is shown that the unstable mode may come from the high or low frequency of the two coupling modes in accordance with the non-proportional damping ratio (see Fig. 9).

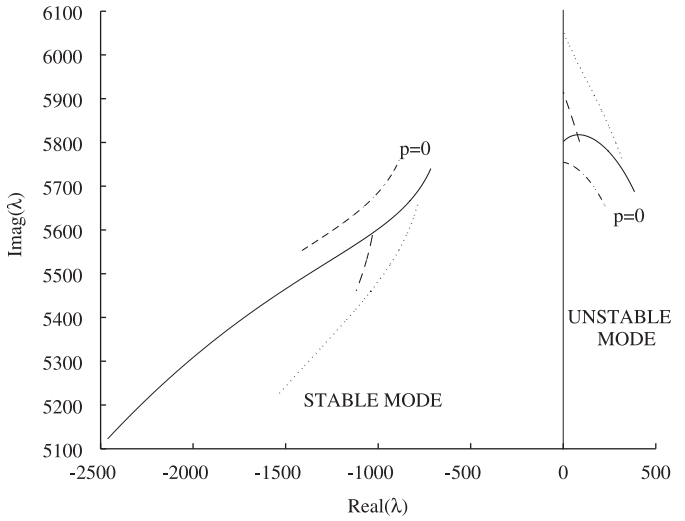

Fig. 9. Evolution of the stable and unstable modes in the complex plane with non-proportional structural damping ($--$ $c_1 = 754\,\mathrm{Nm^{-1}s^{-1}}$ and $c_2 = 1131\,\mathrm{Nm^{-1}s^{-1}}$, $\cdots$ $c_1 = 377\,\mathrm{Nm^{-1}s^{-1}}$ and $c_2 = 565.5\,\mathrm{Nm^{-1}s^{-1}}$, $-$ $c_1 = 377\,\mathrm{Nm^{-1}s^{-1}}$ and $c_2 = 282.75\,\mathrm{Nm^{-1}s^{-1}}$, $-.-$ $c_1 = 754\,\mathrm{Nm^{-1}s^{-1}}$ and $c_2 = 565.5\,\mathrm{Nm^{-1}s^{-1}}$).

Moreover, the role of damping appears to be quite a bit more complicated than in the case of proportional damping. First of all, it may be observed that the smaller limit cycle amplitudes $(X_1, \dot{X}_1)$ and $(X_2, \dot{X}_2)$ are not obtained for the same damping parameters. Then, the addition of non-proportional damping totally changes, the evolution of the real part of the eigenvalue associated with the unstable mode. Fig. 8(a) clearly indicates that the initial value of the real part cannot be used in order to estimate the limit cycle amplitudes. For example, even if the initial real part for case 2 ($c_1 = 377\,\mathrm{Nm^{-1}s^{-1}}$ and $c_2 = 565.5\,\mathrm{Nm^{-1}s^{-1}}$) is higher than the initial real part of case 1 ($c_1 = 754\,\mathrm{m^{-1}s^{-1}}$ and $c_2 = 1131\,\mathrm{Nm^{-1}s^{-1}}$), the associated periodic limit cycles $(X_2, \dot{X}_2)$ are smaller. So it appears that the eigenvalues of the characteristic Eq. (4) cannot be used as a design criterion when the equilibrium point of the mechanical system is unstable. A complex nonlinear analysis and the determination of the self-excited oscillations and the associated limit cycles is needed. Considering these results, it is obvious that structural damping is one of the most important factors for minimizing the limit cycle amplitudes. However, the amount of damping may be correctly chosen in order to avoid bad design. One of the most surprising and fascinating phenomena is that if too much damping is added to only one part of the mechanical system, the size of the limit cycle amplitudes may increase, as illustrated in Fig. 8. Cases 2 and 3 indeed have exactly the same value of damping c_1, but the value of damping c_2 is higher for case 2. Nevertheless, the limit cycles of case 3 are larger than the limit cycles of case 2. So it may be concluded that not only the amount of damping but also the distribution of damping between the two modes are essential.

Moreover, cases 2 and 4 (where c_2 is the same and c_1 is different) show that the limit cycles $(X_1, \dot{X}_1)$ are bigger for case 2, whereas the limit cycles $(X_2, \dot{X}_2)$ are bigger for case 4. So the effects of damping on the limit cycles appear to be very complex and interesting. Using the Complex Nonlinear Modal Analysis, the limit cycles are estimated to be stable.

3.4. *Effects of the cubic nonlinearity on the limit cycles*

In this section, the effects of the cubic nonlinearity on the limit cycles will be studied. First, it should be remembered that the cubic nonlinearity do not influence the stability analysis of the present model due to the fact that the equilibrium point is zero.

Figs. 10 show the variations of the limit cycle amplitudes $(X_1, \dot{X}_1)$ and $(X_2, \dot{X}_2)$ and the evolution of the real and imaginary parts of the unstable mode resulting from the change in the cubic nonlinearity k^{NL} while

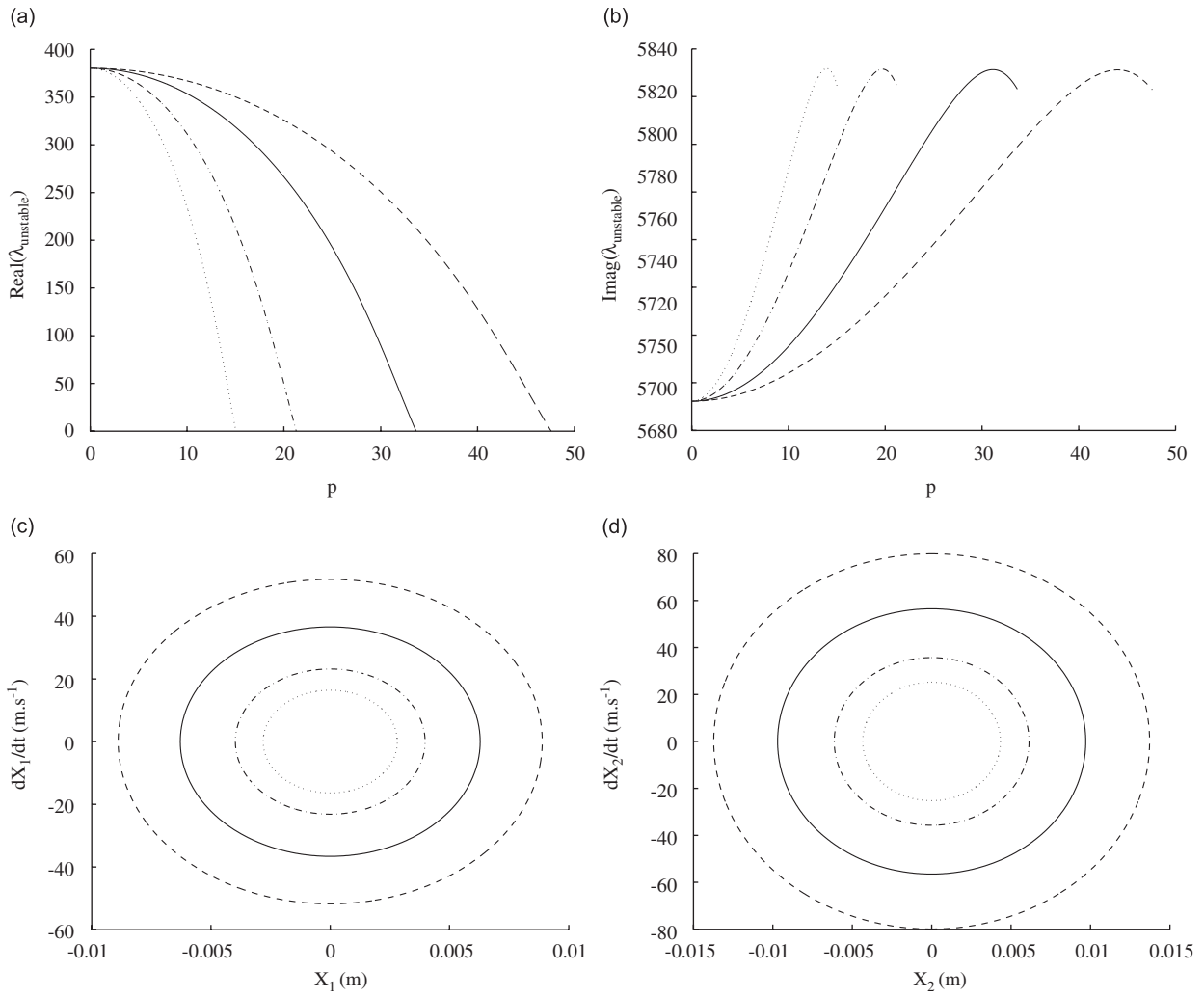

Fig. 10. Evolutions of the unstable mode and the associated limit cycles for $\mu = 0.3$ and $\eta_1 = \eta_2 = 0.06$ (... $k^{NL} = 10^{11}\,N\,m^{-3}$, $-.-$ $k^{NL} = 5.10^{10}\,N\,m^{-3}$,– $k^{NL} = 2.10^{10}\,N\,m^{-3}$, $--$ $k^{NL} = 10^{10}\,N\,m^{-3}$): (a) real parts, (b) associated imaginary part, (c) limit cycles $(X_1, \dot{X}_1)$, and (d) limit cycles $(X_2, \dot{X}_2)$.

keeping the structural damping and other parameters at their initial values (as indicated in Table 1). The effects of the cubic nonlinearity appear very interesting. It may be observed that increasing the nonlinearity decreases the size of the limit cycles. One of the most interesting phenomena is that the evolution form of the imaginary part is the same for the four cases (see Fig. 10(b)). Moreover, the evolution of the unstable mode in the complex plane is exactly the same for the fourth cases, as illustrated in Fig. 11.

3.5. Combined effects of the damping, the friction and the cubic nonlinearity

Figs. 12–14(a) show that the equilibrium point stability of the mechanical system can be altered by changes in the friction coefficient μ, the damping ratio η_2/η_1 and the nonlinearity k^{NL}. It must be emphasized that increasing the friction coefficient (for a given set of parameters) increases the unstable region of the mechanical system (see for example 12(a) and 13(a)). Fig. 12(a) shows that the effects of damping agree with the conclusion of Section 2.2: the more stable system in relation to the structural damping ratio η_2/η_1 corresponds to the equally damped situation (i.e. $c_1 = c_2$ corresponding to $\eta_2/\eta_1 = \omega_{0,1}/\omega_{0,2} = 1.25$).

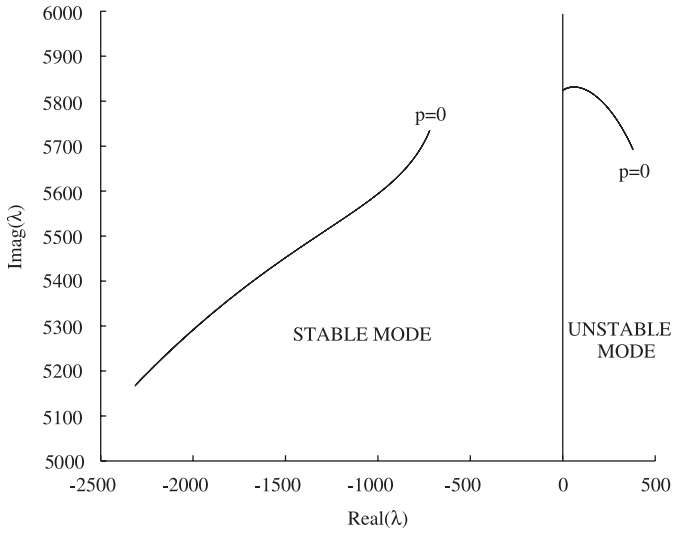

Fig. 11. Evolution of the stable and unstable modes in the complex plane for $\mu = 0.3$ and $\eta_1 = \eta_2 = 0.06$.

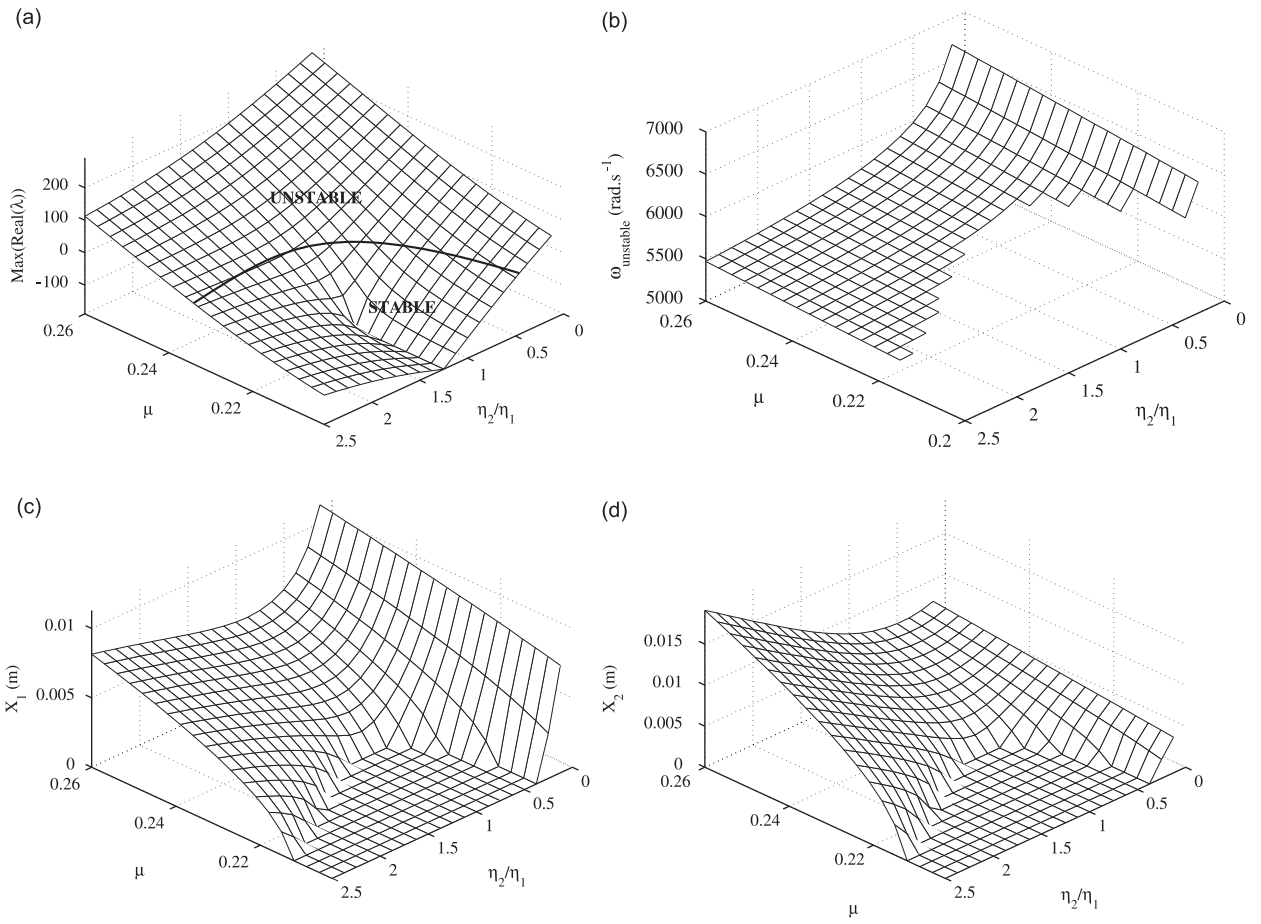

Fig. 12. Amplitudes of the displacements X_1 and X_2 as a function of the friction coefficient μ and the damping ratio η_2/η_1 (with $\eta_1 = 0.06$ and $k^{NL} = 10^{11}\,\mathrm{N\,m^{-3}}$): (a) initial real part for $p = 0$, (b) final frequency, (c) Max(X_1), and (d) Max(X_2).

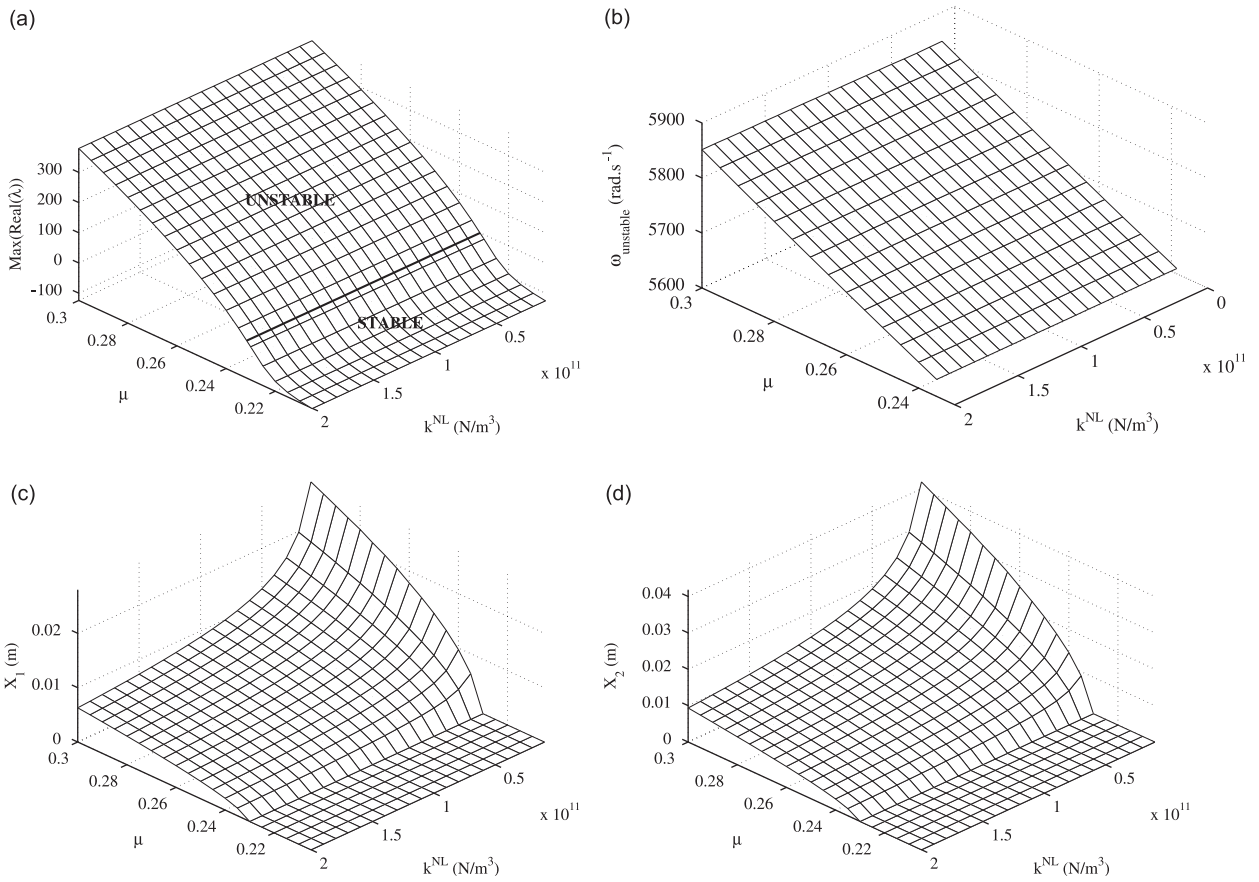

Fig. 13. Amplitudes of the displacements X_1 and X_2 as a function of the friction coefficient μ and the cubic nonlinearity k^{NL} (with $\eta_1 = \eta_2 = 0.06$): (a) initial real part for $p = 0$, (b) final frequency, (c) Max(X_1), and (d) Max(X_2).

In Figs. 13 and 14(a), it appears that the cubic nonlinearity does not influence the stability analysis of the model: as previously explained, the stability analysis is conducted by calculating the Jacobian of the nonlinear system at the equilibrium point [5].

Figs. 12–14(c–d) illustrate the amplitudes of the displacements X_1 and X_2 of the limit cycles when the equilibrium point of the mechanical system is unstable. Performing stability analysis via the Complex Nonlinear Modal Analysis, all the limit cycles appear to be stable. Figs. 12–14(b) give the associated frequency of the self-excited oscillations.

From these parametric studies, we may draw the following general observations for the two-degrees-of-freedom model:

- The effects of structural damping and nonlinearity are important, surprising and interesting phenomena which add another feature in self-exciting mechanisms and flutter instability. Structural damping and the associated structural damping ratio not only influence the stable/unstable zones but also the size of the limit cycles. So, a nonlinear analysis and the determination of the limit cycles are essential in order to avoid worse design and erroneous diagnostics. Special attention has to be paid to the structural damping properties and nonlinear contact of the mechanical systems.
- Neglecting damping or increasing/decreasing damping on only one part of the system may increase the displacement amplitudes X_1 and X_2 of the limit cycles (see Figs. 12).
- We note the existence of a critical value of the friction coefficient after which the equilibrium point of the mechanical system becomes unconditionally unstable. Then, increasing the friction coefficient μ increases the displacement amplitudes X_1 and X_2 of the limit cycles (see Figs. 12 and 13).

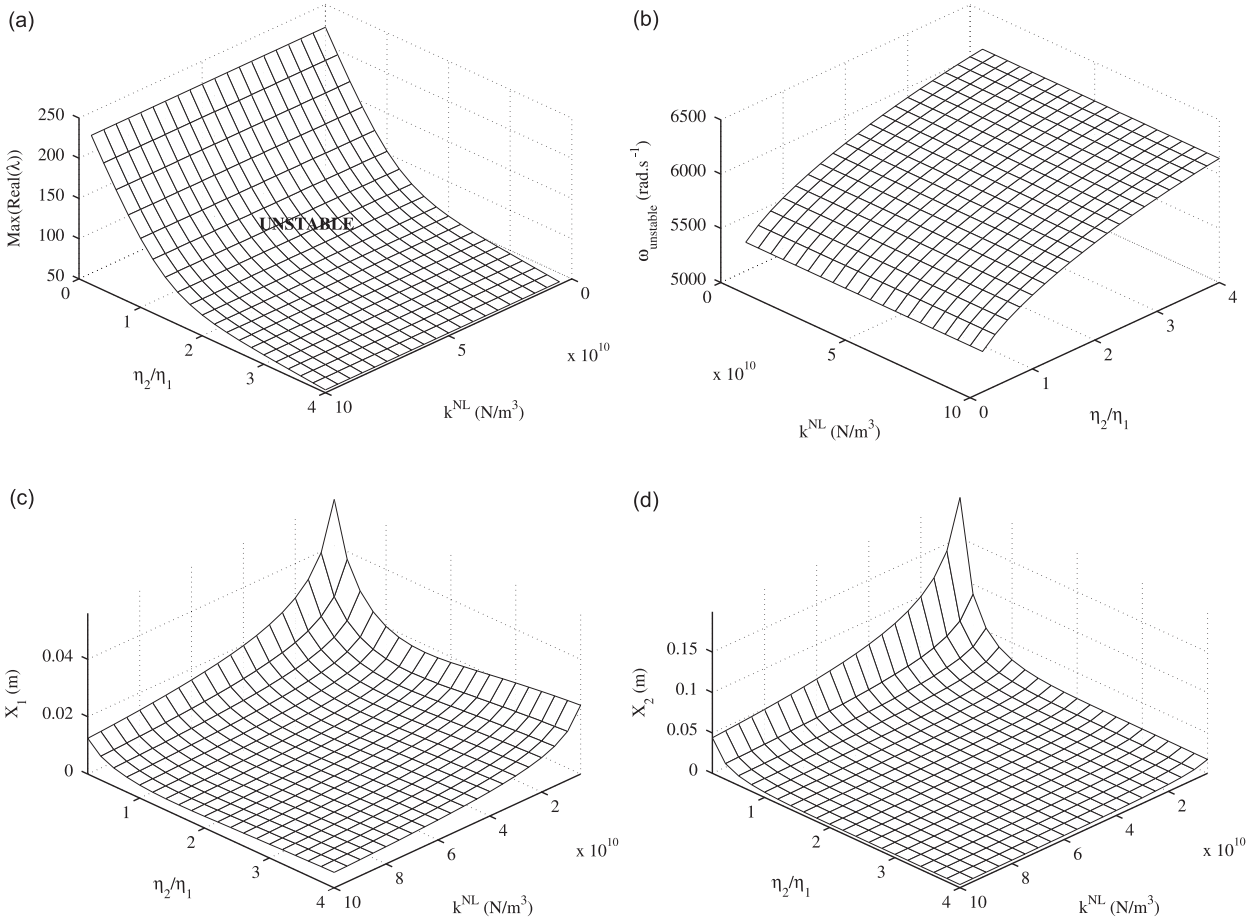

Fig. 14. Amplitudes of the displacements X_1 and X_2 as a function of the damping ratio η_2/η_1 and the cubic nonlinearity k^{NL} (with $\mu = 0.25$ and $\eta_1 = 0.06$): (a) initial real part for $p = 0$, (b) final frequency, (c) Max(X_1), and (d) Max(X_2).

- By increasing the cubic nonlinearity k^{NL}, the displacement amplitudes X_1 and X_2 of the limit cycles decrease (see Figs. 13 and 14).
- One of the most robust (but insufficient) design and compromise solutions to enhance the stable/unstable areas of the mechanical system and to optimize the self-exciting oscillations may be to consider equal structural damping (i.e. $c_1 = c_2$ or $\eta_2/\eta_1 = \omega_{0,1}/\omega_{0,2}$).
- The final frequency of the self-exciting oscillations changes with structural damping, as illustrated in Figs. 12(b) and 14(b).

The same general conclusions have been obtained for the evolution of the velocity amplitudes $\dot{X}_1$ and $\dot{X}_2$.

4. Conclusion

A minimal two-degrees-of-freedom model describing the elementary flutter mechanism of friction-induced vibrations is used to investigate the effects of damping and nonlinearities on flutter instability and the associated limit cycles. It is demonstrated that the commonly accepted idea that ''increasing damping stabilizes a mechanical system or minimizes the self-excited oscillations'' may be wrong. It is shown that the information about the stability of the mechanical system may be erroneous if the undamped mechanical system is used. This study also indicates that the merging scenario and the unstable mode may change the frequency of the

unstable mode. This depends on the structural damping ratio of the two coupling modes that play one of the most important roles in the stable/unstable areas and the size of the limit cycles.

The effects of damping on the limit cycles appear to be complicated and interesting: the amount and distribution of damping may be carefully chosen in order to avoid worse design. A general condition for robust design to enhance the stability of a mechanical system and/or to optimize/minimize the size of limit cycle amplitudes is that proportional structural damping should be added to both modes involved in the mode coupling phenomenon. It was demonstrated that increasing the cubic nonlinearity may decrease the limit cycle amplitudes. It may be concluded that the structural damping ratio between the stable and unstable modes and the nonlinearities are very important and must be taken into account to enhance the stability of mechanical systems or to minimize the amplitudes of self-excited oscillations. Finally, the nonlinear limit cycles and the associated stability of the limit cycles are calculated by applying the Complex Nonlinear Modal Analysis which requires relatively little resources both in terms of the computation time and in terms of the data storage requirements.

Appendix A. Determination of the equilibrium points of the nonlinear system

As indicated in Section 2.2, the equilibrium points $\mathbf{X}_0 = [X_{1,0}\ X_{2,0}]^{\mathrm{T}}$ are obtained by solving the nonlinear static equations

$$\begin{bmatrix} \omega_{0,1}^2 & -\mu\omega_{0,2}^2 \\ \mu\omega_{0,1}^2 & \omega_{0,2}^2 \end{bmatrix} \begin{pmatrix} X_{1,0} \\ X_{2,0} \end{pmatrix} = \begin{pmatrix} -\varphi^{\mathrm{NL}} X_{1,0}^3 \\ -\mu\varphi^{\mathrm{NL}} X_{1,0}^3 \end{pmatrix}. \tag{13}$$

In this study, we assume that the factors $\omega_{0,1}$, $\omega_{0,2}$, φ^{NL} and μ are positive. Firstly, it may be noted that the origin is an equilibrium point of the system.

By premultiplying the second equation of the system (13) by the factor μ, and by comparing the obtained equation with the second equation of the system (13), it follows that the component $X_{1,0}$ verifies

$$X_{1,0}(\omega_{0,1}^2 + \varphi^{\mathrm{NL}} X_{1,0}^2) = 0. \tag{14}$$

Consequently, the equilibrium point components $X_{1,0}$ and $X_{2,0}$ are given by

$$X_{1,0} = 0 \quad \text{and} \quad X_{2,0} = 0 \tag{15}$$

or

$$X_{1,0} = \pm \frac{\mathrm{i}\omega_{0,1}}{\sqrt{\varphi_1^{\mathrm{NL}}}} \quad \text{and} \quad X_{2,0} = 0. \tag{16}$$

So, considering the possible equilibrium points given in Eqs. (15) and (16), it clearly appears that the only physical equilibrium point corresponds to the origin $[X_{1,0}\ X_{2,0}]^{\mathrm{T}} = [0\ 0]^{\mathrm{T}}$.

References

[1] N. Kinkaid, O. O'Reilly, P. Papadopoulos, Automotive disc brake squeal, *Journal of Sound and Vibration* 267 (2003) 105–166.
[2] R. Ibrahim, Friction-induced vibration, chatter, squeal, and chaos. Part 2: dynamics and modeling, *ASME Design Engineering Technical Conferences* 7 (1994) 209–2269.
[3] M. North, A mechanism of disk brake squeal, *14th FISITA Congress*, 1972, paper 1/9.
[4] H. Ouyang, J.E. Mottershead, M.P. Cartmell, M.I. Friswell, Friction-induced parametric resonances in discs: effect of a negative friction velocity relationship, *Journal of Sound and Vibration* 209 (2) (1998) 251–264.
[5] J.-J. Sinou, F. Thouverez, L. Jézéquel, Methods to reduce nonlinear mechanical systems for instability computation, *Archives of Computational Methods in Engineering: State of the Art Reviews* 11 (3) (2004) 257–344.
[6] S. Earles, P. Chambers, Disk brake squeal noise generation: predicting its dependency on system parameters including damping, *International Journal of Vehicle design* 8 (1987) 538–552.
[7] K. Shin, M. Brennan, J.-E. Oh, C. Harris, Analysis of disc brake noise using a two-degree-of-freedom model, *Journal of Sound and Vibration* 254 (2002) 837–848.

[8] N. Hoffmann, L. Gaul, Effects of damping on mode-coupling instability in friction induced oscillations, *ZAMM Zeitschrift fur Angewandti Mathematik und Mechanik* 83 (8) (2003) 524–534.
[9] J.-J. Sinou, L. Jézéquel, Mode coupling instability in friction induced vibrations and its dependency on system parameters including damping, *Journal of European Mechanics—A/Solids* 26 (2007) 106–122.
[10] J.-J. Sinou, F. Thouverez, L. Jézéquel, Stability analysis and nonlinear behaviour of structural systems using the Complex Nonlinear Modal Analysis, *Computers and Structures* 84 (2006) 1891–1905.
[11] J. Hultén, Drum brake squeal: a self-exciting mechanism with constant friction, *SAE Truck and Bus Meeting*, Detroit, Michigan, USA, 1993, paper 932965.
[12] A. Nayfeh, D. Mook, *Nonlinear Oscillations*, Wiley, New York, 1995.
[13] N. Krylov, N.N. Bogoliubov, *Introduction to Nonlinear Mechanics*, Princeton, 1947.
[14] A. D'Souza, A. Dweib, Self-excited vibration induced by dry friction, part 2: stability and limit-cycle analysis, *Journal of Sound and Vibration* 137 (2) (1990) 177–190.
[15] T. Caughey, Equivalent linearization techniques, *The Journal of the Acoustical Society of America* 35 (1963) 1706–1711.
[16] W. Iwan, A generalization of the concept of equivalent Linearization, *International Journal of Nonlinear mechanics* 8 (1973) 279–287.
[17] G. Groll, D.J. Ewins, The harmonic balance method with arc-length continuation in rotor/stator contact problems, *Journal of Sound and Vibration* 241 (2) (2001) 223–233.
[18] G. Somieski, An eigenvalue method for calculation of stability and limit cycles in nonlinear systems, *Nonlinear dynamics* 26 (3) (2001) 3–22.